New Journal of Physics

The open access journal at the forefront of physics

PAPER

CrossMark

Synchronization to extreme events in moving agents

Sayantan Nag Chowdhury[1] ⬩ , Soumen Majhi[1], Mahmut Ozer[2,3], Dibakar Ghosh[1] ⬩ and Matjaž Perc[4,5,6] ⬩

[1] Physics and Applied Mathematics Unit, Indian Statistical Institute, 203 B. T. Road, Kolkata-700108, India
[2] Ministry of National Education, 06420 Ankara, Turkey
[3] Center for Artificial Intelligence and Data Science, Istanbul Technical University, 34469 Istanbul, Turkey
[4] Faculty of Natural Sciences and Mathematics, University of Maribor, Koroška cesta 160, SI-2000 Maribor, Slovenia
[5] Complexity Science Hub Vienna, Josefstädterstraße 39, A-1080 Vienna, Austria
[6] Author to whom any correspondence should be addressed.

E-mail: dibakar@isical.ac.in and matjaz.perc@um.si

Abstract

Interactions amongst agents frequently exist only at particular moments in time, depending on their closeness in space and movement parameters. Here we propose a minimal model of moving agents where the network of contacts changes over time due to their motion. In particular, agents interact based on their proximity in a two-dimensional space, but only if they belong to the same fixed interaction zones. Our research reveals the emergence of global synchronization if all the interaction zones are attractive. However, if some of the interaction zones are repulsive, they deflect synchrony and lead to short-lasting but recurrent deviations that constitute extreme events in the network. We use two paradigmatic oscillators for the description of the agent dynamics to demonstrate our findings numerically, and we also provide an analytical formulation to describe the emergence of complete synchrony and the thresholds that distinguish extreme events from other intermittent states based on the peak-over-threshold approach.

1. Introduction

Research to understand the interplay between complex networks and the dynamical properties of coupled oscillators has been a hotspot for the last few decades and the developing phenomenon of synchronization [1–4] is one of the most important dynamical processes that has been in the center of these researches. Cooperation [5, 6] and time series analysis [7, 8] in complex network have been studied in the past few years. From the perspective of synchronization among coupled oscillators placed into a complex network [9, 10], the correlation between the network's topology and local dynamics is quite decisive. Here, synchronization signifies a process of adaptation to a common collective behavior of oscillators due to their interaction. In most of the previous studies of such systems, the network topology is assumed to be invariant over time and thus the system is controlled by a deterministic static formation for all the course of time. But such a crude assumption regarding the network connectivity inhibits one to model and study most of the practical instances.

Recently, time-varying networks have grabbed the attention of the researchers due to their enormous applications in various fields like functional brain network [11], epidemic modeling [12], communication systems [13, 14] and many more. Time-varying networks, also known as *temporal networks* [15] indicate those networks in which links get activated for a certain course of time. On the assumption of time-invariant nodes which are static over time, many network architecture is studied, e.g. power transmission elements are considered as such nodes among which haphazard links are treated as the coupling between elements of the power transmission system [16]. Even for functional brain networks [11], these types of nodes are considered to characterize the dynamical evolution. Particularly, the scenario of time-varying networks owing to the mobility in the nodes is really a significant platform to study several dynamical processes over them in which nodes can move in the space and interact with each other based on their physical proximity. Collective behavior in random geometric graphs and random walkers has been studied [17, 18]. For instance, in case of coordinated motion of

robots [19], ordered motion in a group of animals [20] and even in the process of chemotaxis [21], this framework has a significant resemblance.

Emergence of complete synchronization from different aspects in temporal networks [22–32], particularly among interacting moving oscillators has been investigated previously [19, 33–41] and most of these articles considered the framework in which each and every agent always carries a vision shape based on which they create neighbors and interact. In this paper, we consider a planar space in which some identical moving chaotic oscillators interact with each other only when they visit the same restricted regions pre-defined in the planar zone. This interactional platform is thus different from most of the existing studies [19, 34–37, 41] in the field on synchronization of moving agents till now, in which each moving agent is associated with an interaction zone that moves with the agent.

Under the setup chosen in this work, we encounter the emergence of complete global synchronization among the moving agents while casting the local dynamical units by two paradigmatic chaotic systems, namely Lorenz [42] and Rössler [43] oscillators, whenever only attractive zones are incorporated inside the planar space. Previously, synchronization has been surveyed [38] from a similar sort of view but nodes in any coupling zone were supposed to interact among each other. But here we are treating this issue differently where the nodes in a particular zone is interacting with each others, but not interacting with any other nodes outside of that coupling zone. In our work, we observe unanticipated abrupt large amplitude deflections from the synchronous regime which is quite different from the usual well-defined formal synchronization state, whenever repulsive zones with suitable strength are included in the space. Such exceptional, rare, repeated large amplitude states signify the incarnation of *extreme events* which are of colossal importance because they can indicate several unexpected natural phenomena. Due to its unanticipated appearance, extreme event delivers a crucial understanding for a variety of fields like share market crashes [44], electric power transmission system [45], earthquakes [46], epileptic seizures in the human brain [47] and many more, though the precise reasoning behind their appearance is yet to be acknowledged. In spite of the fact that there is no general definition of extreme events, such events can be considered as infrequent stochastic events. Existence of such rare though recurrent incidents can be demonstrated by a non-Gaussian probability distribution of amplitudes in a dynamical variable [46, 48, 49]. Extreme events can also be determined whenever the occasional hike of the error from the synchronous manifold crosses a pre-defined threshold. Besides, some researchers are equally interested to unfold the mystery behind its occurrence from the point of view of dynamical systems. In this context, extreme events are observed under the homogeneous network of FitzHugh–Nagumo oscillators coupled with two-time delays [50] due to bubbling transition and blowout bifurcation. Interior crisis, due to the collision of period doubling and a period adding cascade, also leads to extreme events, as reported in the complex networks of FitzHugh–Nagumo units without any influence of noise [51]. Roaming trajectories between various coexisting orbits of varying amplitude under the influence of noise may cause extreme events in a multistable system [52]. Extreme events can also be witnessed along on–off intermitency among coupled chaotic oscillators [53]. Evidence of extreme events in coupled Hindmarsh–Rosebursting neurons interacting through chemical synaptic and gap junctional diffusive coupling is presented in the [54]. Intermittent large deviations of chaotic trajectory indicating the emergence of such rare events in a laser based Ikeda map, has been reported very recently [55].

Here we discuss the synchronization criteria, both analytically and numerically, among the agents moving in a two-dimensional space in which interaction among the moving agents is only possible when they enter the same pre-defined fixed zones. Besides, we observe on–off intermittency in terms of aperiodic switching from the synchronous state as a result of the inclusion of repulsive zones with appropriate strength in the space. More importantly, we present the origination of large amplitude extreme events and discriminate these events from the low-amplitude intermittent states by providing analytical background for the appropriate choice of the extreme event indicator threshold. Non-Gaussian distribution of the spike heights and the temporal away journey of the error beyond the properly justified threshold value are provided as the evidence of the extreme events.

The remaining parts of the paper are assembled as follows. In section 2, we describe the mathematical frame of our model where the network topology varies due to the movement of the agents. Analytical results regarding synchronization are discussed in section 3. Numerical results are shown for the moving oscillators' network using chaotic dynamical systems and we show how the level of synchrony depends upon the parameters like the speed of movement, attractive coupling strength and the number of attractive coupling zones. Section 4 deals with the presence of a repulsive coupling zone and the origination of high amplitude deflections of the network dynamics from the synchronous state signifying the extreme events. Finally, section 5 provides conclusions of our findings.
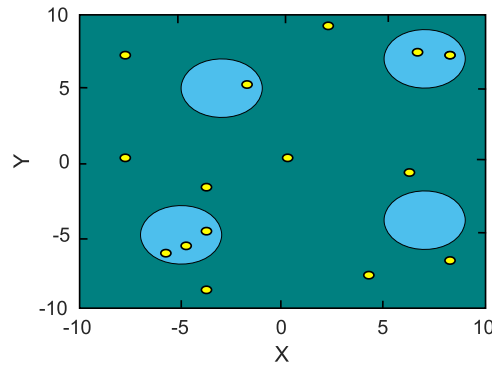
Figure 1. Schematic diagram of a two dimensional space where $N = 15$ agents (smaller yellow circles) are moving independently without any influence of any other agents' motion, in the periodic planar space $\sum = [-g, g] \times [-g, g]$ with $g = 10$. Four disjoint coupling zones (larger circles) are pre-defined in $\sum$. Whenever, the moving individuals enter the same zone, they interact with each other. Note that the agents from one coupling zone do not possess any kind of interaction with the agents belonging to any other coupling zones, they only bother about the members within the same coupling zone, not about the other members of $\sum$.
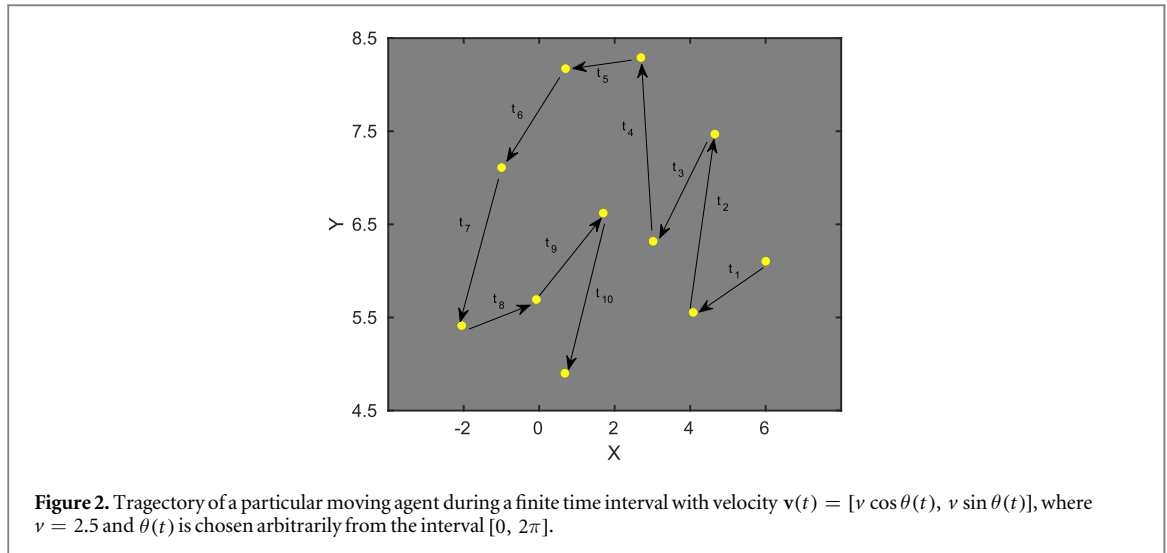
2. Mathematical model for the moving oscillators

We start with describing the mathematical framework of the network model of N moving agents which are distributed in a two dimensional (2D) *XY*-plane $\sum = [-g, g] \times [-g, g]$ of size $L = 4g^2$ sq. units that contain m number of restricted non-overlapping circular zones, each of radius r units. The interactions among the agents are activated only when they enter into the same pre-defined circular zone. In a similar fashion, other types of interaction zones (closed) of square, rectangle or even ellipse shape could have been considered. But, we are considering here simple circular zones, without any loss of generalization (later we show that the analytical condition for synchronization only depends on the area of interaction coupling zone). For illustration, let us consider the upper left interaction coupling zone in figure 1, which contains only one agent (smaller yellow circle). So, this agent cannot interact with any other agents for that particular instant of time. Similarly, the remaining 9 moving agents (outside any coupling zone) in the space $\sum$ are deprived of mutual interaction with that agent and among each other. But for the coupling zone containing 2 agents in the upper right of the figure 1, those two agents are only interacting between themselves for that occasion. The same logic is applicable for the interaction among the 3 moving agents in the lower left coupling zone in the figure. At some time, it may also happen that there will be a zone in which no moving agent is present, e.g. the empty zone in the bottom right.

Now we discuss the scheme of random movement of N agents in the two-dimensional plane. Initially, N identical agents are randomly placed in the region $\sum$. Any kind of bumping collision among those random moving agents is forbidden. The agents are allowed to move in any direction $\theta_i(t)$ with velocity $\mathbf{v}_i(t) = [v \cos \theta_i(t), v \sin \theta_i(t)]$, where v is the modulus of the agent velocity and $\theta_i(t)$, $i = 1, 2, \ldots, N$ are chosen arbitrarily from the interval $[0, 2\pi]$. For better visualization, an exemplary trajectory of a moving agent is depicted graphically in figure 2. To ensure the fact that the moving agents always remain confined within the region $\sum$, the periodic boundary condition is applied. We can relate these moving agents with vehicles equipped with global positioning system device, which enables to track location. The movement of each agent is governed by the dynamical upgrading rule $\mathbf{y}_i(t + \Delta T) = \mathbf{y}_i(t) + \mathbf{v}_i(t)\Delta T$, where $\mathbf{y}_i(t)$ is the position of the ith agent in the plane at any time t and ΔT is the motion integrating step-size. At each integration step, $\theta_i(t)$ and therefore $\mathbf{v}_i(t)$ are updated for the ith agent ($i = 1, 2, \ldots, N$).

Furthermore, a d-dimensional dynamical system is allied with each moving agent. As per the above stated assumptions, the dynamical equation of each agent can be written as

$$\dot{x}^i = F(x^i) - K \sum_{j=1}^{N} g_{ij}(t) H(x^j), \, i = 1, 2, \ldots, N \tag{1}$$

with $x^i(t) = [x_1^i(t), x_2^i(t), \ldots, x_d^i(t)]^T$, $F: \mathbb{R}^d \to \mathbb{R}^d$ given by the system's dynamics, K is the coupling constant, $H(x^j)$ is the vector coupling function for diffusive type of interaction and the time-varying matrix $G(t) = [g_{ij}(t)]_{N \times N}$ is the Laplacian matrix describing the location of all agents and hence the connectivity pattern of the network at any time t with respect to the pre-specified coupling zones. The Laplacian matrix $G(t)$ is defined as a symmetric, positive semi-definite and M-matrix and deliberately calculated as the difference between the degree matrix and the adjacency matrix of the network. Particularly, $g_{ij}(t) = g_{ji}(t) = -1$ if both ith and jth agents enter the same coupling zone at time t, and otherwise zero. Since any kind of self-interaction is intolerable, so we assign $g_{ii}(t) = h$, where h is the number of agents in the same coupling zone at time t, to expect synchronization as one of the possible states of the whole dynamical system. The system given in equation (1) is

Figure 2. Tragectory of a particular moving agent during a finite time interval with velocity $\mathbf{v}(t) = [v \cos \theta(t), \, v \sin \theta(t)]$, where $v = 2.5$ and $\theta(t)$ is chosen arbitrarily from the interval $[0, \, 2\pi]$.

integrated using the Runge–Kutta–Fehlberg method with a fixed time step defined as[7] $\Delta T = 0.01$. The initial conditions are chosen randomly from the phase space where the chaotic attractor resides.

3. Synchronization due to attractive zones

3.1. Analytical condition for synchronization

In this section, we analytically derive the necessary condition for stable synchrony among moving agents in the two-dimensional plane with two attractive interaction zones. As mentioned earlier, synchronization refers to a process in which coupled systems regulate their dynamics to achieve a coherent evolution, and time-averaged Laplacian matrix $\overline{G} = [\overline{g}_{ij}]$ plays a crucial role to understand the synchronization behavior of a time-dependent networked dynamical system. According to the [56], under fast switching among all the possible network configurations, if the system of coupled oscillators given by

$$\dot{x}^i = F(x^i) - K \sum_{j=1}^{N} \bar{g}_{ij} H(x^j), \tag{2}$$

with time-static coupling topology $\bar{G} = [\bar{g}_{ij}]$ goes through stable synchrony and there is a constant λ such that $\frac{1}{\lambda} \int_{t}^{t+\lambda} G(\tau) \mathrm{d}\tau = \bar{G}$, then there exists ϵ_0 such that for all fixed $0 < \epsilon < \epsilon_0$, the system described as

$$\dot{x}^i = F(x^i) - K \sum_{j=1}^{N} g_{ij}(t/\epsilon) H(x^j), \tag{3}$$

(with the time-varying Laplacian $G(t/\epsilon)$) also supports stable synchronization. So if the time-average of the Laplacian matrix $G(t)$, given by $\bar{G} = \frac{1}{\lambda} \int_{t}^{t+\lambda} G(\tau) \mathrm{d}\tau$ exhibits synchrony of the system, then the time varying network will also possess synchronization. The synchronization of the time-evolving network can thus be predicted and assured if the time-averaged network $\overline{G}$ supports synchronization. Henceforth, we now focus to calculate the time-averaged coupling matrix $\overline{G}$.

To simplify the calculations, first we consider two disjoint confined zones with the same area in the physical space $\sum$. Let, $A = \{1, 2, \ldots, N\}$ be the set of all moving agents in the physical space $\sum$ and $B \subseteq A$ be the set of all interacting agents lying within any one of the pre-defined coupling zone and $C \subseteq A$ be another set of all interacting agents lying in any other disjoint pre-defined coupling zone, such that there is no common agents lying in both sets B and C. In other words, $B \cap C = \varnothing$. Let G_B denotes the corresponding Laplacian matrix for the set B and B_i be the resulting sum over all the coupling matrices generated by the ith agent. Let G_A be the zero-row sum Laplacian matrix with $G_A(i, j) = -1$ if $i \neq j$ and $G_A(i, \, i) = N - 1$.

To compute B_i, we consider $j, k \in B \, (j \neq k)$ with cardinality of B equal to i. So, out of $(N - 2)$ agents except the agents j and k, we have to choose $(i - 2)$ elements, which can be done in $\binom{N - 2}{i - 2}$ different ways. Also, we have the off-diagonal entries of G_B as $G_B(j, \, k) = -1$. Then the (j, k)th element of the matrix B_i is

---

[7] The observed results are also surveyed with several different choices of ΔT (not shown here), but perceived results remain unaltered. Thus, we can conclude that the detected observations are independent of the integration time step ΔT.

$$B_i(j, k) = -1 \times \binom{N-2}{i-2}$$

$$= -1 \times \frac{i-1}{N-1} \times \binom{N-1}{i-1}$$

$$= \frac{i-1}{N-1}\binom{N-1}{i-1}G_A(j, k). \tag{4}$$

For diagonal entries of $G_B(k, k)$, where $k \in B$ and with the same assumption that B contains only i agents, we have to deal with $(i-1)$ elements excluding the ith agent, which to be selected out of remaining $(N-1)$ elements. Hence, the diagonal elements of B_i are

$$B_i(k, k) = (i-1)\binom{N-1}{i-1}$$

$$= \frac{i-1}{N-1}\binom{N-1}{i-1}G_A(k, k). \tag{5}$$

Thus, from equations (4) and (5), we can write

$$B_i = \frac{i-1}{N-1}\binom{N-1}{i-1}G_A. \tag{6}$$

Let, out of N moving agents, i individuals go to one restricted zone, while j moving individuals go to another cramp zone. Note that those i agents are completely different from the other j agents and their motion is completely independent from others. Let, p_i be the probability that i agents are coupled with each other. Then, $p_i = P^i(1-P)^{N-i}$, where P is the probability of an agent for lying within a coupling zone. In our case, $P = \frac{\pi r^2}{L}$, where r is the radius of the circular zones. Then the time-averaged matrix becomes

$$\overline{G} = \sum_{i=2}^{N} p_i B_i + \sum_{j=2}^{N-i} p_j B_j$$

$$= \sum_{i=2}^{N} P^i(1-P)^{N-i}\frac{i-1}{N-1}\binom{N-1}{i-1}G_A + \sum_{j=2}^{N-i} P^j(1-P)^{N-i-j}\frac{j-1}{N-i-1}\binom{N-i-1}{j-1}G_A$$

$$= \sum_{i=0}^{N-2} P^{i+2}(1-P)^{N-i-2}\frac{i+1}{N-1}\binom{N-1}{i+1}G_A + \sum_{j=0}^{N-i-2} P^{j+2}(1-P)^{N-i-j-2}\frac{j+1}{N-i-1}\binom{N-i-1}{j+1}G_A$$

$$= P^2 G_A \sum_{i=0}^{N-2} P^i(1-P)^{N-i-2}\binom{N-2}{i} + P^2 G_A \sum_{j=0}^{N-i-2} P^j(1-P)^{N-i-j-2}\binom{N-i-2}{j}$$

$$= P^2 G_A + P^2 G_A$$

$$= 2P^2 G_A. \tag{7}$$

Similarly, we can derive $\overline{G} = mP^2 G_A$ for m disjoint restricted zones with same area. Since, G_A is a zero-sum matrix so that the manifold of synchronous states is neutrally stable, $\overline{G}$ also possesses the same property. Hence, the eigen values of $\overline{G}$ are $\lambda_1 = 0$ and $\lambda_i = mP^2N, i = 2, 3, ..., N$.

Let us now consider the master stability function (MSF) [57, 58] for which stability of the synchronization manifold is assured in the interval $[\alpha, \infty)$, i.e. the MSF $\lambda_{\max}(\alpha)$ is negative only in that given interval $[\alpha, \infty)$.

Hence with the help of the eigen values of $\overline{G}$, we can extract the critical interaction strength K_c for achieving complete synchronization that satisfies $\alpha = mP^2NK_c$ which implies

$$K_c = \frac{\alpha L^2}{m\pi^2 r^4 N}, \tag{8}$$

which is the value of the coupling strength K required to initialize synchronization.

So, whenever K exceeds $\frac{\alpha L^2}{m\pi^2 r^4 N}$, the coupling term provides sufficient amount of coherence among the oscillators to reach synchronization for the whole system.
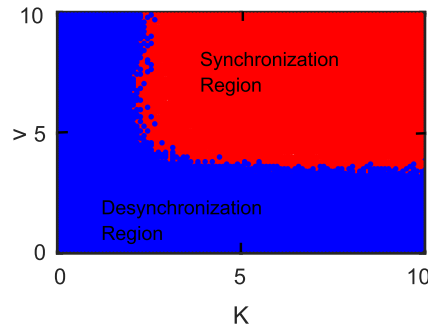
Figure 3. Synchronous behavior in the K–v parameter plane. We set $m = 2$ coupling zones centered at $(g/2, g/2)$ and $(-g/2, -g/2)$, where $g = 10$. The other parameters are fixed at $N = 100$ and $r = 4.0$.

3.2. Numerical findings

In order to look at the dynamical behavior of the network numerically, we first define the synchronization error

$$E = \left\langle \frac{\sum_{i=2}^{N}\sqrt{(x_1^i - x_1^1)^2 + (x_2^i - x_2^1)^2 + (x_3^i - x_3^1)^2}}{(N-1)} \right\rangle_t, \qquad (9)$$

in terms of the standard Euclidean norm, where $\langle\cdots\rangle_t$ stands for time average. Without loss of generality, $H(x^j) = [0, x_2^j, 0]^T$ is taken into consideration as the coupling function. In the following subsections, our attention will be to identify the synchronization region by changing the network parameters, namely the coupling strength K, modulus of velocity v and the number of attractive interaction zones m. We fix the parameters associated with the local dynamics of each individual agent in the chaotic regime.
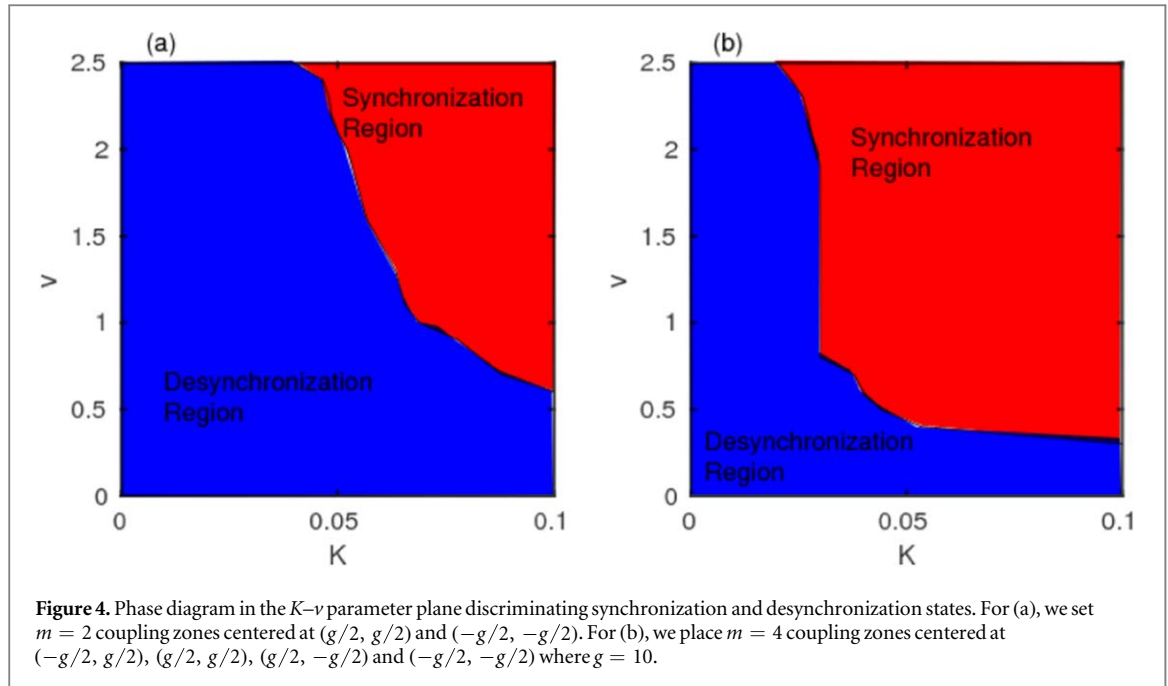
3.2.1. Lorenz system

We first consider the chaotic Lorenz system [42], where the state dynamics of each moving individuals is represented by

$$F(X^i) = \begin{pmatrix} 10(x_2^i - x_1^i) \\ x_1^i(28 - x_3^i) - x_2^i \\ x_1^i x_2^i - \frac{8}{3}x_3^i \end{pmatrix}. \qquad (10)$$

Without loss of any generality, we now meditate on the appearance of synchronization for $N = 100$ identical Lorenz oscillators moving with modulus of velocity $v = 5.0$ and m number of interaction zones of radius $r = 4.0$. We perceive that the synchronization error E descends to zero at $K = 1.0$ and $K = 0.5$ respectively for $m = 2$ and $m = 4$ number of attractive coupling zones, which convey well agreement with the critical interaction strengths $K_c = 0.5$ and $K_c = 1.0$ derived from the relation (8) reflecting the effect of m, for $\alpha = 3.15$. We detect that with the increasing number of interaction zones, the agents can communicate in more space now, as a result of that E decreased to zero more rapidly for larger m.

Here we note that the obtained results remain valid for any other value of the network size N. Particularly, higher N would need lower values of the interaction strength K to achieve synchronization for fixed values of other network parameters (results not shown here). Even that inverse proportional relation between N and K is obvious from equation (8). Since, interaction zones are fixed in plane, mobility of nodes have huge significance in obtaining complete synchronization. On the other hand, the modulus of velocity v does not appear explicitly in the relation (8). So, in order to understand the simultaneous influence of K and v on synchrony, we plot the phase diagram in the K–v parameter space, in figure 3. We affix $m = 2$ interaction zones of radius $r = 4$ in the plane and observe variation in between the parameters K and v for randomly moving oscillators initially in the phase space. We notice that there exists an optimal interval of v for which complete synchronization can be assured depending on the values of the interaction strength K.

Figure 4. Phase diagram in the K–v parameter plane discriminating synchronization and desynchronization states. For (a), we set $m = 2$ coupling zones centered at $(g/2, g/2)$ and $(−g/2, −g/2)$. For (b), we place $m = 4$ coupling zones centered at $(−g/2, g/2)$, $(g/2, g/2)$, $(g/2, −g/2)$ and $(−g/2, −g/2)$ where $g = 10$.

3.2.2. Rössler system

Next we take chaotic Rössler oscillator [43] into consideration which is described as

$$F(X^i) = \begin{pmatrix} -x_2^i - x_3^i \\ x_1^i + 0.2x_2^i \\ 0.2 + x_3^i(x_1^i - 5.7) \end{pmatrix}. \tag{11}$$

With the same number of agents as before, and $v = 2.5$ with $m = 2$ and $r = 4.0$, the synchronization error E with respect to K, drops from a non-zero value to zero at $K_c = 0.039$ and continues to be zero. For the same values of N, m and r with $\alpha = 0.1232$, equation (8) also results in $K_c = 0.039$. Thus our analytical result falls exactly on the results obtained through numerical simulations.
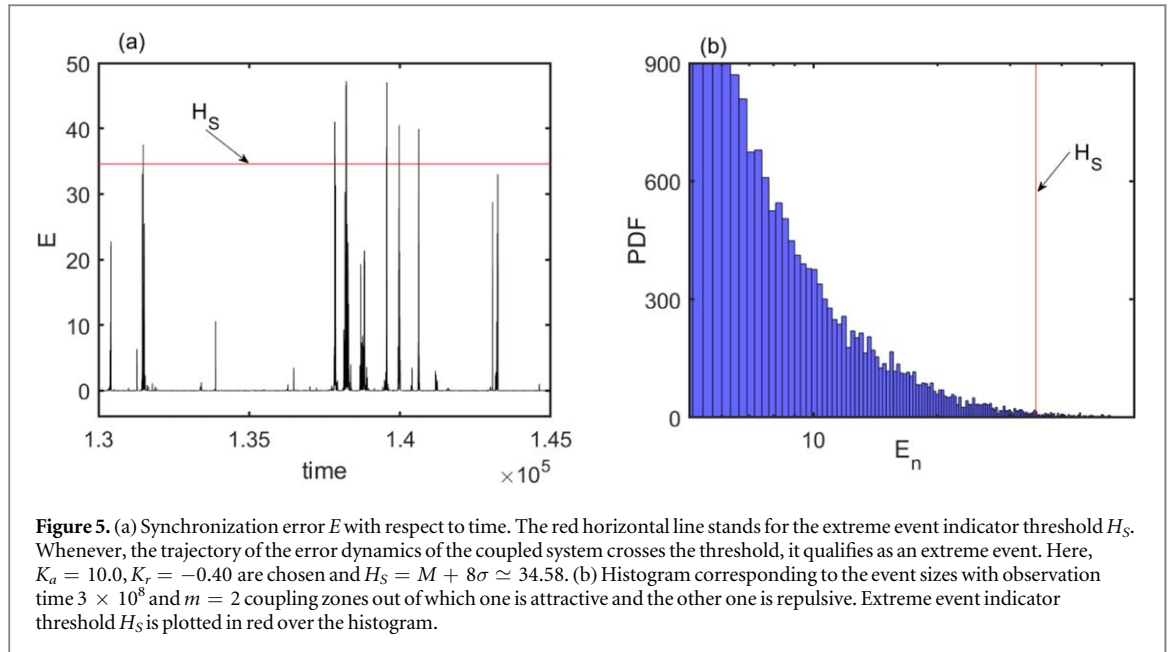
Next, we simultaneously vary the coupling strength K and the modulus v of agents' velocity for different values of m in figure 4. For figure 4(a), we consider two coupling zones of radius $r = 4.0$ as before, centered at $(g/2, g/2)$ and $(−g/2, −g/2)$ and plot the K–v parameter space in terms of the emergence of synchronization. As can be seen, for the whole range of $K \in [0, 0.1]$ and $v \in [0, 2.5]$, the higher the K, the lower the v is needed to achieve synchrony. Next, we add two more attracting coupling zones centered at $(−g/2, g/2)$ and $(g/2, −g/2)$ with all the other parameters fixed as before and plot the K–v parameter space in figure 4(b). A similar sort of behavior as in figure 4(a), is observed here but with a significant enhancement in the synchronization region, as the agents are now able to interact inside two more attracting coupling zones.

4. Inclusion of repulsive coupling zone and emergence of extreme events

Let us now move on to examine the impact of the presence of repulsive zones in the movement space. For this, we will investigate both Lorenz and Rössler oscillators as before.

4.1. Lorenz system

To scrutinize the scenario, two interaction coupling zones centered at $(g/2, g/2)$ and $(g/2, −g/2)$, each of radius $r = 4.0$, are considered on which $N = 100$ identical Lorenz oscillators are randomly moving in any direction with uniform modulus velocity $v = 5.0$. We place the coupling zone centered at $(g/2, g/2)$ as the attractive one and treat the other one as repulsive coupling zone, with K_a and K_r as the attractive and repulsive coupling strengths respectively. Under this arrangement, we spot that the error trajectory continues to be on the invariant synchronous manifold (i.e. $E = 0$) for most of the time, but due to the presence of the repulsive coupling zone with adequate strength, error trajectory experiences non-uniform, uncertain extensive expeditions from the synchronous manifold (see figure 5(a)). This is because the attractor moves near a saddle orbit from where the trajectories get repelled resulting in large excursions. After such deviation, those trajectories come back to the invariant manifold due to stretching and folding nature of chaotic attractors. Such

Figure 5. (a) Synchronization error E with respect to time. The red horizontal line stands for the extreme event indicator threshold H_S. Whenever, the trajectory of the error dynamics of the coupled system crosses the threshold, it qualifies as an extreme event. Here, $K_a = 10.0, K_r = -0.40$ are chosen and $H_S = M + 8\sigma \simeq 34.58$. (b) Histogram corresponding to the event sizes with observation time 3×10^8 and $m = 2$ coupling zones out of which one is attractive and the other one is repulsive. Extreme event indicator threshold H_S is plotted in red over the histogram.

locally repulsive deflection designates on–off intermittent [53, 59] like behavior of the invariant manifold containing nonlinear chaotic orbits. Whenever the error at a certain instant of time crosses the threshold H_S (details discussed later), that event can be considered as an appropriate candidate for extreme events.

To confirm whether the perceived spikes in figure 5(a) reveal the existence of extreme events or not, a sufficiently long time series of the variable E is accumulated and we have constructed a probability density function (PDF) for the event sizes E_n defined as the local maximum values of E. The collected time series is sufficient enough so that due to statistical regularity, inclusion of new sample does not affect the structure of the observed L-shaped PDF [52]. From figure 5(b), it is quite evident that the occurrence of such event sizes is much more than that according to Gaussian distribution and the corresponding histogram possesses a long tail, which guarantees the existence of extreme events.

The presence of events with diverse sizes necessitates to prescribe a criterion that discriminate extreme events from other small-sized events. So, for further characterization of the extremeness, using peak over threshold (POT) approach, we make an attempt based on the specification of a threshold value H_S (say) indicating a significant height that should be crossed by those rare events in order to be counted as an extreme event.

According to the Fisher–Tippet theorem [60] in extreme value theory [61], three types of distributions are mainly used to model the maximum or minimum of the collection of random observations from the same distribution. Specifically, they are the Gumbel, Fréchet, and Weibull distribution [62]. In general, Gumbel and Fréchet distributions correlate with largest extreme value, whereas Weibull model deals with the smallest extreme value [63–65]. Moreover, the Gumbel distribution is unbounded defined on the entire real axis and the Fréchet distribution is bounded for the lower side, $x > 0$ but has a heavy upper tail. So, in seek of the threshold of extreme value indicator, we consider the PDF of a Weibull random variable as follows

$$f(x; \lambda, p) = \begin{cases} \frac{p}{\lambda}\left(\frac{x}{\lambda}\right)^{p-1} e^{-\left(\frac{x}{\lambda}\right)^p} & x \geqslant 0 \\ 0 & x < 0 \end{cases}, \tag{12}$$

where $p > 0$ is the shape parameter and $\lambda > 0$ is the scale parameter of the distribution [65].

Next we proceed by adopting the method developed by Massel [66]. In the asymptotic limit of infinite time observational window, the distribution function can be expressed in terms of Weibull random distribution with $p = 2$ and $\lambda = \sqrt{2}\,\sigma$, i.e. in terms of Rayleigh distribution function

$$f(x; \sigma) = \begin{cases} \frac{x}{\sigma^2} e^{-\frac{x^2}{2\sigma^2}} & x \geqslant 0 \\ 0 & x < 0 \end{cases}, \tag{13}$$

where σ is the the standard deviation of peaks from a time series and under this assumption, the error height H is twice the envelope, that is $H = 2x$ for $x \geqslant 0$. Thus,
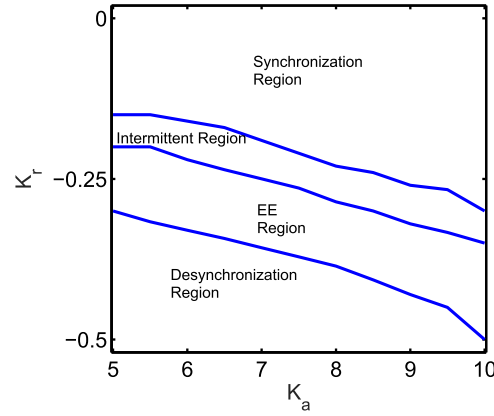
Figure 6. Phase diagram in the K_a–K_r coupling parameters' plane, where regions of synchronization, intermittent, extreme events (EE) and desynchronization are shown. $N = 100$, $\nu = 5.0$ and $m = 2$ coupling zones of radius $r = 4.0$ are chosen out of which one is attractive and the other one is repulsive. Results are obtained from 25 independent numerical realizations, each having 3×10^8 observation time units. Note that, EE region is a subspace of intermittent region having huge deflected spikes of E from the synchronization manifold. A point (K_a, K_r) is included in EE region if and only if it crosses $H_S = M + 8\sigma$ of that time-series.

$$f(H) = \frac{H}{4\sigma^2} e^{-\frac{H^2}{8\sigma^2}}. \tag{14}$$

In 1947, Sverdrup *et al* [67] suggested that the threshold error height H^* should have the probability that exceeds $\frac{1}{3}$, i.e.

$$P(H > H^*) = \frac{1}{3}. \tag{15}$$

Now

$$H^* = \sqrt{\ln 3}\ H_{\mathrm{rms}} = \sigma\sqrt{8\ln 3}, \tag{16}$$

where the root mean square (rms) error height, H_{rms} is defined as square root of the second order moment of the error heights and this H_{rms} can be calculated from the following formula for the kth order moments (about the origin) of the error height:

$$E(H^k) = 2^{\frac{3k}{2}} \sigma^m \Gamma\left(1 + \frac{k}{2}\right). \tag{17}$$

Hence, the effective error height, H_e is defined [68] as

$$\begin{aligned}
\frac{1}{3}H_e &= \int_{H^*}^{\infty} Hf(H)\mathrm{d}H \\
\Rightarrow H_e &= \frac{3}{4} \int_{\sigma\sqrt{8\ln 3}}^{\infty} \frac{H^2}{\sigma^2} e^{-\frac{H^2}{8\sigma^2}}\ \mathrm{d}H \\
&= \left\{ \frac{3\sqrt{\pi}}{2} \mathrm{erfc}\left(\sqrt{\ln 3}\right) + \sqrt{\ln 3} \right\} 2\sqrt{2}\,\sigma.
\end{aligned} \tag{18}$$

Using the error function, H_e can be approximated to 4σ. Then, with the mean M of the errors, extreme events populate the tail of the probability distribution beyond $H_S = M + 2H_e$, i.e. $H_S = M + 8\sigma$. This significant height threshold H_S has been previously used in the context of rogue waves [68–70].

Now, for our network model, we calculate the mean and standard deviation of the error and we have the threshold which is equal to mean plus eight times of the standard deviation calculated over the time interval as in figure 5(a). We set this threshold as a horizontal line (red line) in the figure 5(a) plotted over the variation of error with respect to time.

In figure 6, we identify different dynamical states, namely synchronization, intermittent spikes, extreme events as a consequence of on–off intermittent states and desynchronization states in the K_a–K_r coupling parameter space within the ranges $K_a \in [5, 10]$ and $K_r \in [-0.55, 0.0]$. We particularly demonstrate the sensitivity of the negative coupling parameter K_r on the network dynamics. For smaller values of K_r, the attractive interactions dominate and the networked system maintains complete synchronization for suitable optimal values of K_a. However, as soon as K_r becomes higher, we need much higher K_a to retain synchrony, otherwise, with increasing K_r depending on K_a, the synchronization becomes intermittent and gradually generate extreme events. This scenario is depicted through the EE region in the phase diagram. If we continuously increase K_r, the synchrony gets completely deflected producing desynchronization.
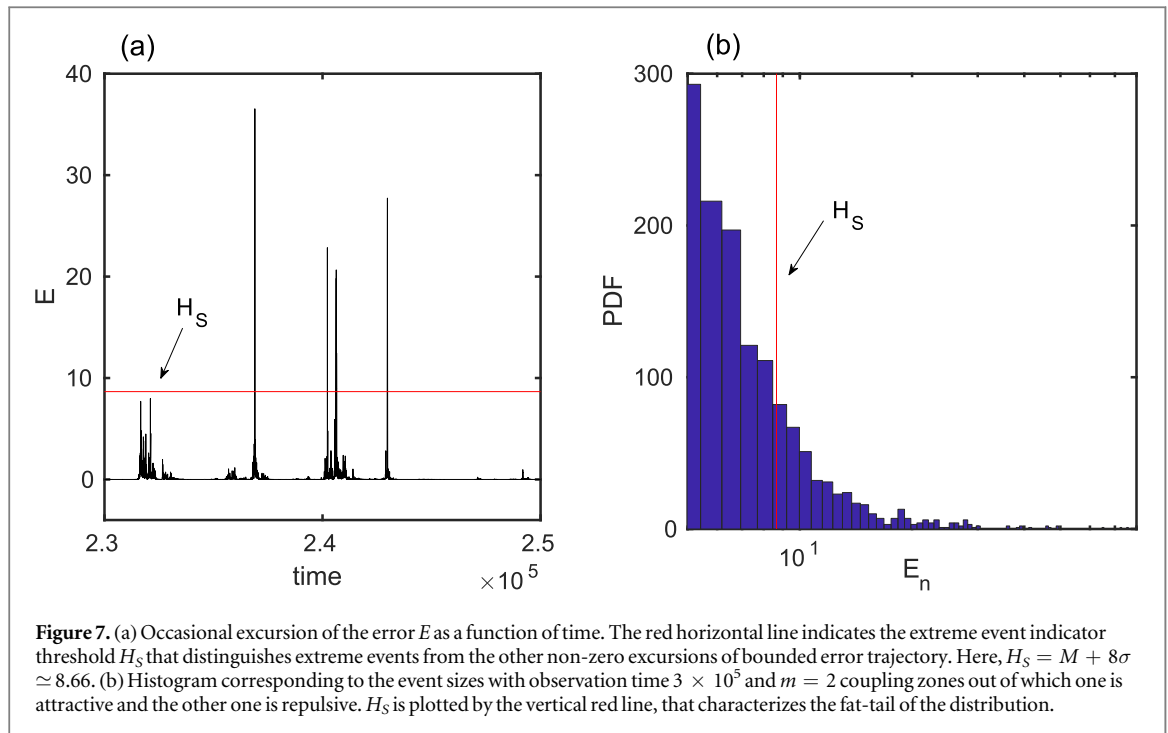
Figure 7. (a) Occasional excursion of the error E as a function of time. The red horizontal line indicates the extreme event indicator threshold H_S that distinguishes extreme events from the other non-zero excursions of bounded error trajectory. Here, $H_S = M + 8\sigma$ $\simeq 8.66$. (b) Histogram corresponding to the event sizes with observation time 3×10^5 and $m = 2$ coupling zones out of which one is attractive and the other one is repulsive. H_S is plotted by the vertical red line, that characterizes the fat-tail of the distribution.

4.2. Rössler oscillators

Again, we inspect the influence of the presence of a repulsive zone in the movement space by keeping fixed Rössler oscillators in each of these moving agents. We fix one attracting coupling zone centered at $(g/2, g/2)$ and one repulsive coupling zone centered at $(g/2, -g/2)$, each of same radius $r = 4.0$, having the same area. Under this framework, $N = 100$ Rössler oscillators, with modulus velocity $v = 2.5$, display high amplitude fluctuation from the synchronous manifold (see figure 7(a)) for attractive coupling strength $K_a = 1.0$ and repulsive coupling strength $K_r = -0.1$. As discussed earlier, the chaotic dynamics of the network was confined to the original synchronization manifold as long as the coupling zones provide attractive interactions. But whenever along with attractive zone the movement space consists of a zone bringing appropriate repulsive force, the synchronization becomes intermittent and the dynamical network occasionally blows out of the manifold.

On–off intermittency in the form of aperiodic switching among the synchronous state (i.e. when the error is zero) and chaotic eruption of the oscillation is observed in the error dynamics (see figure 7(a)). Whenever the error at a certain instant of time crosses the threshold H_S, that event can be considered as an appropriate candidate for extreme events. The spikes observed here are recurrent, aperiodic and of different amplitudes indicating the origination of extreme events. For a better understanding of this scenario, in figure 7(b), the histogram associated to the PDF of the event sizes is plotted from a sufficiently long time series of the dynamical units where E_n stands for local maximum values of E (see equation (9)). We observe non-Gaussian (L-shaped) distribution of the events in the semi-log scale [52], that clarifies the occurrence of events with heterogeneously distributed sizes and hence of the extreme events.

In a similar fashion, we observed extreme events while considered different numbers of attractive or repulsive coupling zones (figures not shown here) and the inclusion of repulsive coupling zones are identified as necessary in order to realize extreme events.

5. Discussions and conclusions

In most of the previous works [50–55], the studies on extreme events are done either by considering only single isolated dynamical system or by considering static dynamical network formalisms and the possible temporal evolution of the network itself are rather ignored. But, dynamical systems in nature are rarely isolated and more importantly, in most of the cases interacting dynamical units in physical, biological and social networks undergo through time-varying connections instead of being coupled via static regular topologies. In contrast, we here have explored the phenomenon of synchronization together with its deflection towards the emergence of extreme events, based on fundamental principles of motion and network science, in a time-evolving model of interaction among moving agents, where each individual is moving in a two-dimensional plane with some pre-existing coupling zones. The agents are allowed to interact with each other only when they move into the same coupling zone. The study of extreme events [71] have received less attention, although discovery of definitive

extreme events indicating threshold is highly desirable for its scientific understanding, particularly for the problems, such as earthquakes, epileptic seizures and social dynamics, where the governing equations are unknown. Extreme events on complex networks play an important role due to its wide possible applications on dynamical processes. The analysis of extreme events can also help in the management of disease, for example to prevent sudden outbreaks. For instance, our study may be beneficial to avoid extreme events in many human-made systems, e.g. reduction of overusage of antibiotics, which causes worsening medical cost and mortality especially for life-threatening bacteria infections [72]. Chen *et al* already showed that hysteresis can appear as an unprecedented roadblock for the recovery of vaccination uptake [73]. Our perceived study may be also useful to understand this puzzling phenomenon too.

In order to authorize our results, we successfully dealt with two well known chaotic systems, Lorenz and Rössler oscillators. The emergence of synchronization in this described time-varying complex network is thoroughly investigated in presence of only attractive coupling zones. Parameter regions for the synchronization state have been figured out by varying modulus velocity v of the moving oscillators for different number of coupling zones m. Numerically, it is shown that the modulus velocity v of the moving agents plays a crucial role in order to obtain synchronization of the system. The interval of interaction strength that induces synchrony has also been estimated analytically. Besides, extreme event like behavior deflecting the synchronization manifold is observed in the network whenever the repulsive coupling zone with effective strength has been introduced in the physical space. Non-Gaussian distribution of the event size is identified that explains the emergence of the extreme events.

In this paper, extreme events are considered as those short lasting events characterized by

- unpredictable appearance with respect to time due to random mechanism with very low probability,

- having amplitudes higher than $H_S = M + 8\sigma$, and

- they appear much more often than they would according to Gaussian statistics [74].

The extreme value distribution obtained through block extrema approach demands an extensive sequence of data to conclude robust interpretation. This complication is somehow controlled to some extent using peak over threshold approach by considering a suitable extreme event indicating threshold depending on their probabilities of occurrence or on the point where they have potential consequences.

Next, we provide a proper justification for the choice of the threshold value that distinguishes extreme events from the usual intermittency in synchrony, and with the help of this threshold value, the occurrence of the extreme events are established. We have also been able to map the dynamical states of synchronization and extreme events in the parameter plane of the attractive and repulsive interaction strengths, which points out to the fact that mere inclusion of repulsive zones may preserve stable synchrony region or induce intermittent behavior or even purely desynchronization region, but not necessarily extreme events. To obtain extreme events like phenomena, the proper choice of both coupling parameters is crucial. This also sheds light to the fact that proper choice of both coupling parameters can help the system push away from extreme events, which helps to mitigate extreme events.

Acknowledgments

ORCID iDs

Sayantan Nag Chowdhury ⓘ https://orcid.org/0000-0002-0326-826X
Dibakar Ghosh ⓘ https://orcid.org/0000-0003-4832-5210
Matjaž Perc ⓘ https://orcid.org/0000-0002-3087-541X

References

[1] Arenas A, Díaz-Guilera A, Kurths J, Moreno Y and Zhou C 2008 *Phys. Rep.* **469** 93
[2] Pikovsky A, Rosenblum M and Kurths J 2003 *Synchronization: A Universal Concept in Nonlinear Science* (Cambridge: Cambridge University Press)
[3] Boccaletti S, Kurths J, Osipov G, Valladares D L and Zhou C S 2002 *Phys. Rep.* **366** 1
[4] Gómez-Gardenes J, Moreno Y and Arenas A 2007 *Phys. Rev. Lett.* **98** 034101
[5] Khoo T, Fu F and Pauls S 2016 *Sci. Rep.* **6** 36293

[6] Fu F and Chen X 2017 *New J. Phys.* **19** 071002

[7] Gao Z K, Small M and Kurths J 2016 *Europhys. Lett.* **116** 50001

[8] Dang W, Gao Z K, Lv D, Liu M, Cai Q and Hong X 2018 *New J. Phys.* **20** 125005

[9] Barabási A L 2016 *Network Science* (Cambridge: Cambridge University Press)

[10] Berec V 2017 *Euro. Phys. J. Spec. Top.* **226** 2205

[11] Valencia M, Martinerie J, Dupont S and Chavez M 2008 *Phys. Rev.* E **77** 050905(R)

[12] Stehle J, Voirin N, Barrat A, Cattuto C, Colizza V, Isella L, Regis C, Pinton J F, Khanafer N and Vanhems P 2011 *BMC Med.* **9** 87

[13] Onnela J P, Saramaki J, Hyvonen J, Szabo G, Lazer D, Kaski K, Kertesz J and Barabasi A L 2007 *Proc. Natl Acad. Sci. USA* **104** 7332

[14] Wu Y, Zhou C, Xiao J, Kurths J and Schellnhuber H J 2010 *Proc. Natl Acad. Sci. USA* **107** 18803

[15] Holme P and Saramäki J 2012 *Phys. Rep.* **519** 97

[16] Sachtjen M L, Carreras B A and Lynch V E 2000 *Phys. Rev.* E **61** 4877

[17] Díaz-Guilera A, Gómez-Gardenes J, Moreno Y and Nekovee M 2009 *Int. J. Bifurcation Chaos* **19** 687

[18] Guo Q, Cozzo E, Zheng Z and Moreno Y 2016 *Sci. Rep.* **6** 37641

[19] Buscarino A, Fortuna L, Frasca M and Rizzo A 2006 *Chaos* **16** 015116

[20] Buhl J, Sumpter D J T, Couzin I D, Hale J J, Despland E, Miller E R and Simpson S J 2006 *Science* **312** 1402

[21] Tanaka D 2007 *Phys. Rev. Lett.* **99** 134103

[22] Kohar V, Ji P, Choudhary A, Sinha S and Kurths J 2014 *Phys. Rev.* E **90** 022812

[23] Rakshit S, Majhi S, Bera B K, Sinha S and Ghosh D 2017 *Phys. Rev.* E **96** 062308

[24] Gross T and Blasius B 2008 *J. R. Soc. Interface* **5** 259

[25] Rakshit S, Bera B K, Ghosh D and Sinha S 2018 *Phys. Rev.* E **97** 052304

[26] Belykh I V, Belykh V N and Hasler M 2004 *Physica* D **195** 188

[27] Majhi S and Ghosh D 2017 *Europhys. Lett.* **118** 40002

[28] Skufca J D and Bollt E M 2004 *Math. Biosci. Eng.* **1** 347

[29] Rakshit S, Bera B K and Ghosh D 2018 *Phys. Rev.* E **98** 032305

[30] Ito J and Kaneko K 2001 *Phys. Rev. Lett.* **88** 028701

[31] Ren W, Beard R W and Atkins E M 2007 *IEEE Control Syst. Mag.* **27** 71

[32] Nag Chowdhury S and Ghosh D 2019 *Europhys. Lett.* **125** 10011

[33] Uriu K, Morishita Y and Iwasa Y 2010 *Proc. Natl Acad. Sci. USA* **107** 4979

[34] Frasca M, Buscarino A, Rizzo A and Fortuna L 2012 *Phys. Rev. Lett.* **108** 204102

[35] Frasca M, Buscarino A, Rizzo A, Fortuna L and Boccaletti S 2008 *Phys. Rev. Lett.* **100** 044102

[36] Fujiwara N, Kurths J and Díaz-Guilera A 2011 *Phys. Rev.* E **83** 025101

[37] Majhi S and Ghosh D 2017 *Chaos* **27** 053115

[38] Kim B, Do Y and Lai Y C 2013 *Phys. Rev.* E **88** 042818

[39] Porfiri M M, Stilwell D, Bollt E M and Skufca J D 2006 *Physica* D **224** 102

[40] Porfiri M, Stilwell D J, Bolt E M and Skufca J D 2006 *Physica* D **224** 102

[41] Majhi S, Ghosh D and Kurths J 2019 *Phys. Rev.* E **99** 012308

[42] Lorenz E N 1963 *J. Atmos. Sci.* **20** 130

[43] Rössler O E 1976 *Phys. Lett.* A **57** 397

[44] Feigenbaum J A 2001 *Quant. Finance* **1** 346

[45] Dobson I, Carreras B A, Lynch V E and Newman D E 2007 *Chaos* **17** 026103

[46] Sornette D and Quillon G 2012 *Eur. Phys. J. Spec. Top.* **205** 1

[47] Albeverio S, Jentsch V and Kantz H 2010 *Extreme Events in Nature and Society* (Berlin: Springer)

[48] Sornette D 2002 *Proc. Natl Acad. Sci. USA* **99** 2522

[49] Kim J W and Ott E 2003 *Phys. Rev.* E **67** 026203

[50] Saha A and Feudel U 2017 *Phys. Rev.* E **95** 062219

[51] Ansmann G, Karnatak R, Lehnertz K and Feudel U 2013 *Phys. Rev.* E **88** 052911

[52] Pisarchik A N, Reategui R J, Escoboza R S, Cuellar G H and Taki M 2011 *Phys. Rev. Lett.* **107** 274101

[53] Cavalcante H L D S, Oriá M, Sornette D, Ott E and Gauthier D J 2013 *Phys. Rev. Lett.* **111** 198701

[54] Mishra A, Saha S, Vigneshwaran M, Pal P, Kapitaniak T and Dana S K 2018 *Phys. Rev.* E **97** 062311

[55] Ray A, Rakshit S, Ghosh D and Dana S K 2019 *Chaos* **29** 043131

[56] Stilwell D J, Bollt E M and Roberson D G 2006 *SIAM J. Appl. Dyn. Syst.* **5** 140

[57] Pecora L M and Carroll T L 1998 *Phys. Rev. Lett.* **80** 2109

[58] Huang L, Chen Q F, Lai Y C and Pecora L M 2009 *Phys. Rev.* E **80** 036204

[59] Pradas M, Tseluiko D, Kalliadasis S, Papageorgiou D T and Pavliotis G A 2011 *Phys. Rev. Lett.* **106** 060602

[60] Fisher R A and Tippett L H C 1928 *Proc. Camb. Phil. Soc.* **24** 180

[61] Lucarini V, Faranda D, Freitas A C, Freitas J M, Holland M, Kuna T, Nicol M, Todd M and Vaienti S 2016 *Extremes and Recurrence in Dynamical Systems* (New York: Wiley)

[62] Nicolis C, Balakrishnan V and Nicolis G 2006 *Phys. Rev. Lett.* **97** 210602

[63] Kotz S and Nadarajah S 2000 *Extreme Value Distributions: Theory and Applications* (London: Imperial College Press)

[64] Gumbel E J 1958 *Statistics of Extremes* (New York: Columbia University Press)

[65] Weibull W 1951 A statistical distribution function of wide applicability *J. Appl. Mech.* **18** 293

[66] Massel S R 1996 *Ocean Surface Waves: Their Physics and Prediction* (Singapore: World Scientific)

[67] Sverdrup H U and Munk W H 1947 Wind, sea and swell : theory of relations for forecasting *Technical Report* University of California (https://doi.org/10.5962/bhl.title.38751)

[68] Kharif C, Pelinovsky E and Slunyaev A 2009 *Rogue Waves in the Ocean* (Berlin: Springer)

[69] Dysthe K, Krogstad H E and Müller P 2008 *Annu. Rev. Fluid Mech.* **40** 287

[70] Bonatto C, Feyereisen M, Barland S, Giudici M, Masoller C, Leite J R R and Tredicce J R 2011 *Phys. Rev. Lett.* **107** 053901

[71] Farazmand M and Sapsis T P 2019 *Appl. Mech. Rev.* (https://doi.org/10.1115/1.4042065)

[72] Chen X and Fu F 2018 *Front. Phys.* **6** 139

[73] Chen X and Fu F 2019 *Proc. R. Soc.* B **286** 20182406

[74] Akhmediev N and Pelinovsky E 2010 *Eur. Phys. J. Spec. Top.* **185** 1